



Published in final edited form as:

Nature. 2009 August 27; 460(7259): 1145–1148. doi:10.1038/nature08285.

Immortalization eliminates a roadblock during cellular reprogramming into iPS cells

Jochen Utikal^{1,2,3,*}, Jose M. Polo^{1,2,*}, Matthias Stadtfeld^{1,2}, Nimet Maherali^{1,2,4}, Warakorn Kulalert^{1,2}, Ryan M. Walsh^{1,2}, Adam Khalil^{1,2}, James G. Rheinwald⁵, and Konrad Hochedlinger^{1,2,#}

¹Massachusetts General Hospital Cancer Center and Center for Regenerative Medicine; Harvard Stem Cell Institute; 185 Cambridge Street, Boston, MA, 02114, USA

²Department of Stem Cell and Regenerative Biology, Harvard University, Cambridge, MA 02138, USA

³Department of Dermatology, Venereology and Allergology, University Medical Center Mannheim, Ruprecht-Karl-University of Heidelberg, Theodor-Kutzer-Ufer 1-3, 68135 Mannheim, Germany

⁴Department of Molecular and Cellular Biology, Harvard University; 7 Divinity Avenue, Cambridge, MA 02138, USA

⁵Department of Dermatology, Brigham and Women's Hospital and Harvard Skin Disease Research Center, 77 Avenue Louis Pasteur, Boston, MA 02115, USA

Abstract

The overexpression of defined transcription factors in somatic cells results in their reprogramming into induced pluripotent stem (iPS) cells^{1–3}. The extremely low efficiency and slow kinetics of *in vitro* reprogramming suggest that additional rare events are required to generate iPS cells. The nature and identity of these events, however, remain elusive. We noticed that the reprogramming potential of primary fibroblasts into iPS cells decreases upon serial passaging and the concomitant onset of senescence. Consistent with the notion that loss of replicative potential provides a barrier for reprogramming, we here demonstrate that cells with low endogenous ARF levels and immortal fibroblasts deficient for components of the p16INK4a/ARF/p53 pathway yield iPS colonies with a 3-fold faster kinetics and at a significantly higher efficiency compared with wild-type (WT) cells, endowing almost every somatic cell with the potential to form iPS cells. Importantly, acute genetic ablation of p53 in cellular subpopulations that normally fail to reprogram rescues their ability to produce iPS cells. Our results show that the acquisition of immortality is a crucial and rate-limiting step towards the establishment of a pluripotent state in somatic cells and underscore the similarities between pluripotent cell lines and tumor cells.

#corresponding author (khochedlinger@helix.mgh.harvard.edu).

*equally contributing authors

Author contributions

J.U., J.M.P. and K.H. conceived the study, interpreted results and wrote the manuscript, J.U. and J.M.P. performed the majority of experiments with help from W.K., R.W. and A.K. M.S., N.M. and J.G.R. provided essential study material and helped with interpretation of results.

The possibility to generate patient-specific pluripotent cells may enable the study and treatment of multiple degenerative diseases and therefore has enormous therapeutic potential. A major limitation of inducing pluripotency, however, is its low efficiency, which ranges between 0.01–0.2% when using direct viral infection of adult cells with vectors expressing the reprogramming factors Oct4, Sox2, Klf4 and cMyc^{2,4–6} and reaches up to 3% when using optimized “secondary systems”^{7–9}; secondary systems are based on somatic cells that already carry all four reprogramming genes in their genome under the control of doxycycline-inducible elements, thus enabling homogeneous transgene expression (Suppl. Fig. 1). The low efficiency of reprogramming secondary cells suggests the requirement for additional molecular events that restrict the conversion of somatic cells into iPS cells¹. Identifying these restrictions is critical for understanding the mechanisms of induced pluripotency as well as for its potential clinical applications.

We noticed that secondary murine embryonic fibroblasts (MEFs) at early passages generate iPS cells more efficiently than MEFs at later passages, consistent with the notion that a high replicative potential of somatic cells is critical for successful reprogramming into iPS cells (Fig. 1a, top panel). The accumulation of β -galactosidase-positive senescent cells in late passage cultures further suggests that molecular changes associated with cellular senescence provide a roadblock for the conversion of somatic cells into iPS cells (Fig. 1a, bottom panel). Loss of replicative potential is often the consequence of culture-induced upregulation of the cell cycle inhibitors p16INK4a, ARF and p21Cip1 as well as activation of p53¹⁰. Indeed, we observed a progressive upregulation of *p16INK4a*, *ARF* and *p21Cip1* transcript levels in serially passaged MEFs (Fig. 1b). Growth of MEFs in low oxygen (4%) can counteract culture-induced upregulation of p16INK4a/ARF/p53, thereby extending replicative lifespan (Fig. 1c)¹¹. We detected a 3-fold increase in reprogramming efficiency in secondary MEFs cultured in low oxygen (Fig. 1d, e), in agreement with the notion that p16INK4a and activated p53 inhibit reprogramming.

To directly test if the expression status of the *INK4a/ARF* locus in the starting cell population has an influence on reprogramming, we analyzed cells derived from an ARF-GFP knock-in reporter mouse¹². ARF-GFP MEFs at passage 3 contained a population of ARF-GFP^{high} and ARF-GFP^{low} cells, consistent with previous observations¹² (Fig. 1f). Interestingly, FACS-purified ARF-GFP^{low} MEFs yielded iPS colonies twice as efficiently as ARF-GFP^{high} MEFs, indicating that reduced ARF levels in the starting cell population are beneficial for reprogramming (Fig. 1g, h).

Notably, ARF-GFP expression was undetectable and endogenous *p16INK4a* and *ARF* transcript levels were downregulated in established iPS cells (Fig. 2a and Suppl. Fig. 2a), further indicating that inactivation of this key senescence pathway by the reprogramming factors may be critical for the acquisition of pluripotency. In agreement, expression of the four reprogramming factors for six days resulted in efficient downregulation of the ARF-GFP allele (Fig. 2a). However, no single reprogramming factor alone was sufficient to silence ARF-GFP expression (Fig. 2a), suggesting that the synergistic action of at least two of the factors is required to inhibit *INK4a/ARF* transcription.

To examine how silencing of the *INK4a/ARF* locus correlates with other markers that change during reprogramming, we followed the expression of ARF-GFP in intermediate cell populations previously identified by surface markers^{13,14}. Interestingly, *INK4a/ARF* expression was downregulated specifically in the Thy1⁻ and SSEA1⁺ fractions, which are enriched for cells poised to become iPS cells, but not in the Thy1⁺ fraction, which fails to give rise to iPS cells (Fig. 2b). p16INK4a RNA and protein levels followed a similar trend as the arf-GFP expression during reprogramming (Suppl. Fig. 3). Interestingly, SSEA1⁺ ARF-GFP^{low} cells had a 3-fold higher reprogramming potential than SSEA1⁺ ARF-GFP^{high} cells, indicating that low ARF expression is a useful prospective marker to further enrich for intermediate cells poised to become iPS cells (Fig. 2c, d). Together, these results show that downregulation of the *INK4a/ARF* locus correlates well with, and further refines previously identified subpopulations of cells undergoing reprogramming.

Using a published PCR-based assay¹⁵, we found that iPS cells and ES cells, in contrast to MEFs, show *INK4a/ARF* promoter methylation, consistent with stable transcriptional silencing of *INK4a/ARF* in pluripotent cells (Suppl. Fig. 2b). However, the downregulation of ARF-GFP expression at day 6 of reprogramming as seen by FACS (Fig. 2b) was not yet accompanied by detectable promoter methylation, suggesting that stable silencing of the *INK4a/ARF* locus is a late event during reprogramming that requires additional molecular changes. In agreement with a transient decrease of *ARF* expression, withdrawal of doxycycline from day 6 cultures resulted in the rapid reappearance of ARF-GFP expression and the failure to recover stable iPS colonies (Fig. 2b and data not shown). Promoter methylation became first detectable at day 9 of reprogramming specifically in the SSEA1⁺ fraction (Suppl. Fig. 2b), which contains the majority of stably reprogrammed cells¹³. This observation indicates that the stable silencing of the *INK4a/ARF* locus is achieved by epigenetic modifications and occurs specifically in late intermediate cells that are poised to become iPS cells.

Since genetic deletion of the *INK4a/ARF* locus in fibroblasts results in their immortalization¹⁶, we wondered whether immortalized somatic cells are more amenable to reprogramming than primary cells. We first assessed the reprogramming potential of a spontaneously immortalized melanocyte line¹⁷ (designated “Melan A”). Melan A cells gave rise to iPS cells four times more efficiently compared with primary melanocytes, yielding efficiencies close to 1% (Fig. 3a, Suppl. Fig. 3a–d). Injection of iPS cells into SCID mice gave rise to well-differentiated teratomas, and introduction into blastocysts yielded chimeric mice that showed contribution to different tissues (Fig. 3b, c, Suppl. Fig. 4e). These results document that an established cell line remains permissive for reprogramming into a pluripotent state. Spontaneous immortalization of cultured cells is usually accompanied by mutations of components of the p53 or *INK4a/ARF* pathways¹⁸. Indeed, Western blot analysis revealed the absence of p16INK4a protein in Melan A cells (Suppl. Fig. 4f) even though sequence analysis of the *p16INK4a* and *ARF* exons did not reveal any mutations (data not shown).

To assess a more accurate reprogramming frequency of immortalized vs. primary melanocytes, we established secondary cells through *in vitro* differentiation of iPS cells^{7,8} (Suppl. Fig. 1, Suppl. Fig. 5a). Secondary cells obtained from primary melanocytes

converted into iPS cells at an average efficiency of 1.5%, consistent with previous observations^{7-9,19} (Fig. 3d, clones 1-3). Remarkably, however, Melan A-derived secondary cells gave rise to iPS cells at efficiencies of up to ~65%, indicating that immortalization endows almost 2 in 3 cells with the potential to form iPS cells (Fig. 3d, clones 57-61, Suppl. Fig. 5b). Moreover, single-cell sorting of one subclone (clone 59.3) generated iPS cells at 100% efficiency, demonstrating that most, if not all, of the cells have acquired the potential to undergo reprogramming under optimal conditions (Fig. 3e). Secondary MEFs obtained from Melan A-iPS cells at embryonic day (E) 14.5 gave rise to iPS cell colonies at an efficiency of ~40%, which is comparable to *in vitro*-derived secondary cells (Fig. 3d, clones M4 and M5).

We next tested if deletion of *p53* or *INK4a/ARF* in fibroblasts mimicks the phenotype of spontaneously immortalized cells. Indeed, we observed a 30-40-fold increase in the number of iPS cell colonies in *p53*, *INK4a/ARF* and *ARF* mutant cells compared with WT control cells, demonstrating that inactivation of these pathways is likely responsible for the increased reprogramming efficiencies of spontaneously immortalized cells (Fig. 3f, Suppl. Fig. 6, Suppl. Table 1). Moreover, *p53*^{-/-} iPS cell-derived E14.5 secondary MEFs gave rise to iPS cell colonies at an efficiency of ~80%, similar to results obtained with spontaneously immortalized cells (Fig. 3g). Collectively, these observations provide strong functional evidence that the inactivation of key pathways controlling replicative potential and senescence substantially enhance the reprogramming potential of somatic cells into iPS cells.

To exclude the possibility that an altered growth rate of immortal cells rather than their long-term proliferation potential influences their increased reprogramming potential, we compared the iPS cell formation efficiencies of *p53*^{-/-} and WT MEFs grown under low (0.5% FBS) and high (15% FBS) serum conditions. *p53*-deficient MEFs cultured in low serum exhibited a significantly reduced growth rate compared with MEFs cultured in high serum (Suppl. Fig. 7a). In spite of this growth disadvantage, *p53*-mutant cells gave rise to iPS cells more efficiently than WT MEFs, suggesting that the long-term proliferation potential of immortal cells is responsible for their enhanced reprogramming potential (Suppl. Fig. 67, c).

Given that the acquisition of immortality through downregulation of *INK4a/ARF* or *p53* appears to eliminate a roadblock during the reprogramming of somatic cells into iPS cells, inactivation of these pathways should also affect the kinetics of reprogramming. Indeed, while WT cells required 8 days of transgene expression to produce stable iPS cells, which is consistent with previous reports^{13,14}, *p53* and *INK4a/ARF* mutant cells gave rise to iPS colonies after only 3 and 4 days of transgene expression, respectively, demonstrating that the acquisition of cellular immortality is not only an efficiency-limiting but also a rate-limiting step during induced pluripotency (Fig. 3h).

Surprisingly, we failed to detect a correlation between the relative numbers of Thy1⁻ and SSEA1⁺ intermediate cells and reprogramming efficiency in *p53*^{-/-} over WT cultures (Suppl. Fig. 7). This suggests that immortal cells undergoing reprogramming pass through the same roadblocks as control cells but that immortality endows those cells that otherwise

fail to reprogram with the potential to form iPS cells. To further test this hypothesis, we plated FACS-purified Thy1⁺, Thy1⁻ and SSEA1⁺ cells isolated from WT or *p53*-deficient secondary cells on feeders in the presence or absence of doxycycline (Fig. 4a). In WT cells, iPS cells appeared predominantly from the SSEA1⁺ population at all time points and to a lesser degree from the Thy1⁻ and Thy1⁺ fractions in the continuous presence of doxycycline (Fig. 4a, left graph). However, when doxycycline was withdrawn after sorting of these populations, only the SSEA1⁺ fraction at day 9 gave rise to stable iPS cells, consistent with previous observations^{13,14} (Fig. 4a, right graph). This result is in accordance with the earlier finding that methylation of the *INK4a/ARF* locus becomes detectable specifically in the SSEA1⁺ population in WT cells (Suppl. Fig. 2b). In contrast, *p53*-deficient secondary cells continuously treated with doxycycline gave rise to iPS cells at high efficiency and regardless of Thy1 and SSEA1 expression status (Fig. 4a, left graph). Moreover, when doxycycline treatment was discontinued after sorting, iPS cell colonies emerged from Thy1⁺, Thy1⁻ and SSEA1⁺ cells as early as 3 days after induction of transgenes. These findings confirm that reprogramming kinetics are up to three times faster in immortal cells compared with primary cells and demonstrate that *p53* deficiency confers reprogramming potential upon cells that normally fail to form iPS cells.

Since continuous *p53* deficiency in MEFs may select for genomic aberrations that favor reprogramming into iPS cells, we acutely inhibited p53 expression by infecting secondary WT cells with a lentiviral construct expressing a short hairpin against p53 (shp53)²⁰. We found that MEFs treated with shp53 at any time point during reprogramming give rise to iPS cell colonies at higher efficiency compared with control cells (Fig. 4b). Furthermore, infection of Thy1⁺ and Thy1⁻ cells with shp53 yielded iPS cells at similar efficiencies as the SSEA1⁺ population, demonstrating that acute inactivation of p53 is sufficient to confer the ability to undergo reprogramming on cells that would otherwise fail to form iPS cells (Fig. 4c). Likewise, the treatment of senescent cultures, which appear refractory to reprogramming, with shp53 rescued their ability to produce iPS cells (Suppl. Fig. 9). Importantly, we demonstrate a continuous requirement for the absence of p53 to elicit an enhanced effect on reprogramming using a Cre-activatable allele of p53 (Suppl. Fig. 10).

Lastly, we sought to determine if human immortalized cells are equally amenable to reprogramming as murine cells. To this end, we compared the reprogramming abilities of primary and hTERT-immortalized human keratinocyte cell lines, which show comparable growth rates but obvious differences in their long-term proliferation potential²¹. Indeed, hTERT-immortalized keratinocyte lines gave rise to iPS-like colonies ~20 times more efficiently compared with early passage cultures of the primary keratinocyte line, which they were derived from (strain N)²¹, indicating that overcoming replicative senescence is critical during the reprogramming of both murine and human somatic cells into iPS cells (Suppl. Fig. 11).

Our results indicate that the acquisition of immortality through epigenetic silencing of the *INK4a/ARF* locus provides a bottleneck for the conversion of somatic cells into iPS cells, thus contributing to the low efficiency and delayed kinetics of *in vitro* reprogramming. Upon immortalization of fibroblasts, however, almost every somatic cell (or its clonal offspring) is endowed with the potential to generate iPS cells (Fig. 4d). Our findings are consistent with

previous reports showing a more subtle effect of genetically interfering with immortalization pathways on iPS cell formation efficiency in human cells^{22,23}. Since p53 and INK4a/ARF are guardians of chromosomal stability, however, their manipulation in a therapeutic setting should be approached with caution. Primary cell populations with low endogenous levels of p53 or p16INK4a/ARF^{24–26} or cells with a high endogenous proliferative potential, such as somatic stem and progenitor cells²⁷, might provide an alternative and safer source for producing iPS cells at high efficiency.

Materials and Methods

Viral vectors and production

The generation and structure of replication-defective doxycycline-inducible lentiviral vectors and a lentiviral vector constitutively expressing the reverse tetracycline-controlled transactivator (rtTA) has been described in detail elsewhere^{13,28}. Viral supernatant was concentrated approximately 100-fold by ultracentrifugation at 20,000 rpm for 1.5 hours at 4°C, resuspended in 300 µl PBS, and stored at –80°C. Infections were carried out in 1 ml medium using 5 µl of each viral concentrate per 35mm plate.

Cell culture and in vitro differentiation of iPS cells

Melan A cells were grown in RPMI medium containing 10% FCS and 200 nM TPA¹⁷. Melan A cells were single cell cloned and only one subclone was used for subsequent experiments. Fibroblast cultures containing a reactivatable p53 allele as well as the ROSA26-CreER allele²⁹ were obtained from the tail of an adult mouse as described previously¹³. p53^{–/–} fibroblasts as well as INK4A/ARF^{–/–} murine embryonic fibroblasts (MEFs) were cultured in DMEM containing 10%FCS. Primary melanocytes were purchased from the Skin Diseases Research Center, Yale School of Medicine and were grown like Melan A cells. For lentiviral vector infections, cells were seeded in 6 well plates at a density of 1×10^5 cells/well and infected on 3 consecutive days. Medium changes were performed 12–24 h after infection. One day after the last infection, ES cell medium containing 1 µg/ml doxycycline was added. Fresh ES cell medium with doxycycline was added every other day until iPS cell colonies developed. Five days later, cell culture conditions were switched to ES cell medium in the absence of doxycycline. iPS cell colonies were picked into 96-well cells containing PBS without magnesium and calcium using a 10 µl pipette. Trypsin was added to each well, incubated for 5 minutes and single cell suspension was transferred into 24-well dishes containing MEF feeder layers. Picked iPS cells were grown on MEFs in standard ES cell conditions. For blastocyst injections, iPS cells were marked with a FUGW lentiviral vector constitutively expressing GFP. For in vitro differentiation assays, iPS cells were grown in the absence of LIF on uncoated plates to induce embryoid body formation. Embryoid bodies were explanted on gelatinized plates and outgrowths were dissociated by trypsinization and expanded for FACS purification (see flow cytometry).

Human cell culture and generation of human iPS cells

The human epidermal keratinocyte lines strain N, N/TERT-1, and N/TERT-2G were grown in K-sfm medium as previously described²¹. STEMCCA lentiviral vector²⁸ infections were carried out with human keratinocytes in 6 well plates at a density of 100,000 cells/well on 2

subsequent days. The infection efficiency of primary human keratinocytes after 2 subsequent infections with tetO-GFP lentiviral vector in the presence of the rtTA expressing lentiviral vector was 40%. Medium changes were performed 12 h after infections and 1 day after infection human keratinocytes were transferred to MEFs. Media containing 50% keratinocyte medium and 50% human ES cell medium containing 0.5 µg/ml doxycycline was added one day later. Medium changes were performed every other day in the presence of 0.5 µg/ml doxycycline until iPS cell colonies developed. Upon appearance of human ES cell-like colonies, medium was switched to human ES cell culture conditions and human iPS cells were picked and further expanded as described previously⁸.

Calculation of reprogramming efficiencies

For cells directly infected with lentivirus (LV-tetO-Oct4, -Sox2, -Klf4 and -cMyc¹³ plus FUGW-rtTA¹³, or LV-tetO-STEMCCA²⁸ plus FUGW-rtTA), reprogramming efficiencies were calculated based on the infection efficiency of somatic cells with a single control virus expressing EGFP (FUGW-GFP) or by performing immunofluorescence for Oct4 and Sox2. For secondary cells, equal numbers of cells were plated in the absence or presence of doxycycline on 100mm dishes coated with gelatin or containing a layer of irradiated MEF feeders. Efficiencies were determined on average 20 days later by dividing the number of iPS colonies that grew after withdrawal of doxycycline by the number of seeded cells or, alternatively, by the number of colonies that adhered on the control plate in the absence of doxycycline.

Alkaline phosphatase (AP) staining

AP staining was performed using an Alkaline Phosphatase substrate kit (Vector laboratories) according to manufacturer's recommendations.

Immunofluorescence

iPS cells were cultured on pretreated coverslips, fixed with 4% PFA, and permeabilized with 0.5% Triton X-100. The cells were then stained with primary antibodies against mOct4 (Santa Cruz, sc-8628), mSox2 (Chemicon, AB5603), and mNanog (Abcam, ab21603). Respective secondary antibodies were conjugated to Alexa Fluor 546 (Invitrogen). Nuclei were counterstained with DAPI (Invitrogen). Cells were imaged with a Leica DMI4000B inverted fluorescence microscope equipped with a Leica DFC350FX camera. Images were processed and analyzed with Adobe Photoshop software.

Flow cytometry

Harvested cells were incubated with antibodies against Thy1.2 (PE conjugated, 53-2.1, eBiosciences), SSEA-1 (mouse IgM, MC-480, Developmental Hybridoma Bank) and Flk1 (biotinylated, Aves 12a1, eBiosciences) for 20 minutes. Cells were washed in PBS and then incubated for 20 minutes with APC conjugated anti mouse IgM, (eBioscience) and Pacific Blue-conjugated streptavidin (Invitrogen). The cells were washed in PBS, resuspended in propidium iodide 5% FBS/PBS solution and passed through a 40µm cell strainer to achieve single cell suspension. Cells positive for Thy1 and Flk1 and negative for SSEA1 were sorted

on a FACSAria (BD Biosciences). For analysis and/or sorting of intermediates, cells were stained with Thy1.2 and SSEA1 antibodies and sorted or analyzed as indicated.

PCR analysis

For quantitative PCR (qPCR) analysis, RNA was isolated from cells with the TRIzol reagent (Invitrogen). For strongly pigmented cells an additional phenol/chloroform purification step was performed before RNA clean up with the RNeasy Minikit (Qiagen). cDNA was produced with the Super Script III kit (Invitrogen). Real-time quantitative PCR reactions were set up in triplicates with the Brilliant II SYBR Green QPCR Master Mix (Stratagene) and run on a Mx3000P QPCR System (Stratagene). Primer sequences are listed in Supplemental Table 2. Genotyping for the p53 $-/-^*$ allele was performed by PCR using the following 3 primer pairs: P53K_A: CAAACTGTTCTACCTCAAGAGCC, P53K_B: AGCTAGCCACCATGGCTTGAGTAAGTCTGCA P53K_C: CTTGGAGACATAGCCCACTG (kindly provided by Dr. A. Ventura).

Western blot analysis

Cell extracts were run in 15% SDS-PAGE gels. The gels were run at 90V until proteins were separated (~ 2 hours) and transferred to PVDF membranes (Bio-Rad) by running overnight at 20V, 4°C in transfer apparatus (Bio-Rad). The membranes were washed in PBS-T (PBS + 0.1% Tween) and blocked in 5% milk in PBS-T for one hour. The membranes were then incubated with anti-p16INK4A, anti-p53 (phospho s15) (abcam) and γ -tubulin antibody overnight at 4°C, washed and incubated in horseradish peroxidase-conjugated anti-rabbit antibodies for 1 hour at room temperature. Immunoblots were then visualized using ECL reagent (Santa Cruz).

Cellular senescence detection

Cellular senescence was detected using a cellular senescence detection kit (Millipore) based on β -Gal staining according to manufacturer's recommendations.

Bisulfite sequencing

Bisulfite treatment of DNA was performed with the EpiTect Bisulfite Kit (Qiagen) according to manufacturer's instructions. Primer sequences were as previously described for Oct4 and Nanog⁴. Amplified products were purified by using gel filtration columns, cloned into the pCR4-TOPO vector (Invitrogen), and sequenced with M13 forward and reverse primers.

Generation of teratomas and chimeras

For teratoma induction, 2×10^6 cells of each iPS cell line were injected subcutaneously into the dorsal flank of isoflurane-anesthetized SCID mice. Teratomas were recovered 3–5 weeks postinjection, fixed overnight in 10% formalin, paraffin embedded, and processed with hematoxylin and eosin. For chimera production, female BDF1 mice were superovulated with PMS (pregnant mare serum) and hCG (human chorion gonadotropin) and mated to BDF1 stud males. Zygotes were isolated from plugged females 24 h after hCG injection. After 3 days of in vitro culture in KSOM media, blastocysts were injected with iPS cells, and

transferred into day2.5 pseudopregnant recipient females. C-sections were performed 17 days later and pups were fostered with lactating females.

Supplementary Material

Refer to Web version on PubMed Central for supplementary material.

Acknowledgments

We thank Drs. Martine Roussel and Charles Sherr for generously providing us with ARF-GFP cells, Drs. Dorothy C Bennett and Elena Sviderskaya for sharing Melan A cells and Drs. Andrea Ventura and Tyler Jacks for tail biopsies of conditional p53 mutant mice. We also thank Drs. Alex Tsatsos and Nabeel Bardeesy for valuable suggestions, for critical reading of the manuscript and for providing INK4a/ARF^{-/-} MEFs. J.U. was supported by a postdoctoral fellowship from the Mildred Scheel Foundation, J.M.P. by an ECOR fellowship and M.S. by a fellowship from the Schering Foundation. J.G.R. was supported by an NIH Skin Disease Research Center Grant. NM was supported by a graduated scholarship from the Natural Sciences and Engineering Council of Canada. Support to K.H. came from the NIH Director's Innovator Award, the Harvard Stem Cell Institute, the Kimmel Foundation and the V Foundation.

References

1. Hochedlinger K, Plath K. Epigenetic reprogramming and induced pluripotency. *Development*. 2009; 136:509–23. [PubMed: 19168672]
2. Takahashi K, et al. Induction of pluripotent stem cells from adult human fibroblasts by defined factors. *Cell*. 2007; 131:861–72. [PubMed: 18035408]
3. Takahashi K, Yamanaka S. Induction of pluripotent stem cells from mouse embryonic and adult fibroblast cultures by defined factors. *Cell*. 2006; 126:663–76. [PubMed: 16904174]
4. Maherali N, et al. Directly reprogrammed fibroblasts show global epigenetic remodeling and widespread tissue contribution. *Cell Stem Cell*. 2007; 1:55–70. [PubMed: 18371336]
5. Okita K, Ichisaka T, Yamanaka S. Generation of germline-competent induced pluripotent stem cells. *Nature*. 2007; 448:313–7. [PubMed: 17554338]
6. Wernig M, et al. In vitro reprogramming of fibroblasts into a pluripotent ES-cell-like state. *Nature*. 2007; 448:318–24. [PubMed: 17554336]
7. Hockemeyer D, et al. A drug-inducible system for direct reprogramming of human somatic cells to pluripotency. *Cell Stem Cell*. 2008; 3:346–53. [PubMed: 18786421]
8. Maherali N, et al. A high-efficiency system for the generation and study of human induced pluripotent stem cells. *Cell Stem Cell*. 2008; 3:340–5. [PubMed: 18786420]
9. Wernig M, et al. A drug-inducible transgenic system for direct reprogramming of multiple somatic cell types. *Nat Biotechnol*. 2008; 26:916–24. [PubMed: 18594521]
10. Collado M, Blasco MA, Serrano M. Cellular senescence in cancer and aging. *Cell*. 2007; 130:223–33. [PubMed: 17662938]
11. Parrinello S, et al. Oxygen sensitivity severely limits the replicative lifespan of murine fibroblasts. *Nat Cell Biol*. 2003; 5:741–7. [PubMed: 12855956]
12. Zindy F, et al. Arf tumor suppressor promoter monitors latent oncogenic signals in vivo. *Proc Natl Acad Sci U S A*. 2003; 100:15930–5. [PubMed: 14665695]
13. Stadtfeld M, Maherali N, Breault DT, Hochedlinger K. Defining molecular cornerstones during fibroblast to iPS cell reprogramming in mouse. *Cell Stem Cell*. 2008; 2:230–40. [PubMed: 18371448]
14. Brambrink T, et al. Sequential Expression of Pluripotency Markers during Direct Reprogramming of Mouse Somatic Cells. *Cell Stem Cell*. 2008; 2:151–159. [PubMed: 18371436]
15. Sharpless NE, et al. Loss of p16Ink4a with retention of p19Arf predisposes mice to tumorigenesis. *Nature*. 2001; 413:86–91. [PubMed: 11544531]
16. Serrano M, et al. Role of the INK4a locus in tumor suppression and cell mortality. *Cell*. 1996; 85:27–37. [PubMed: 8620534]

17. Bennett DC, Cooper PJ, Hart IR. A line of non-tumorigenic mouse melanocytes, syngeneic with the B16 melanoma and requiring a tumour promoter for growth. *Int J Cancer*. 1987; 39:414–8. [PubMed: 3102392]
18. Kamijo T, et al. Tumor suppression at the mouse INK4a locus mediated by the alternative reading frame product p19ARF. *Cell*. 1997; 91:649–59. [PubMed: 9393858]
19. Hanna J, et al. Direct reprogramming of terminally differentiated mature B lymphocytes to pluripotency. *Cell*. 2008; 133:250–64. [PubMed: 18423197]
20. Ventura A, et al. Cre-lox-regulated conditional RNA interference from transgenes. *Proc Natl Acad Sci U S A*. 2004; 101:10380–5. [PubMed: 15240889]
21. Dickson MA, et al. Human keratinocytes that express hTERT and also bypass a p16(INK4a)-enforced mechanism that limits life span become immortal yet retain normal growth and differentiation characteristics. *Mol Cell Biol*. 2000; 20:1436–47. [PubMed: 10648628]
22. Mali P, et al. Improved efficiency and pace of generating induced pluripotent stem cells from human adult and fetal fibroblasts. *Stem Cells*. 2008; 26:1998–2005. [PubMed: 18511599]
23. Zhao Y, et al. Two supporting factors greatly improve the efficiency of human iPSC generation. *Cell Stem Cell*. 2008; 3:475–9. [PubMed: 18983962]
24. Molofsky AV, et al. Increasing p16INK4a expression decreases forebrain progenitors and neurogenesis during ageing. *Nature*. 2006; 443:448–52. [PubMed: 16957738]
25. Krishnamurthy J, et al. p16INK4a induces an age-dependent decline in islet regenerative potential. *Nature*. 2006; 443:453–7. [PubMed: 16957737]
26. Janzen V, et al. Stem-cell ageing modified by the cyclin-dependent kinase inhibitor p16INK4a. *Nature*. 2006; 443:421–6. [PubMed: 16957735]
27. Eminli S, et al. Differentiation stage determines reprogramming potential of hematopoietic cells into iPSC cells. *Nature Genetics*. (in press).
28. Sommer CA, et al. iPSC Cell Generation Using a Single Lentiviral Stem Cell Cassette. *Stem Cells*. 2008
29. Ventura A, et al. Restoration of p53 function leads to tumour regression in vivo. *Nature*. 2007; 445:661–5. [PubMed: 17251932]

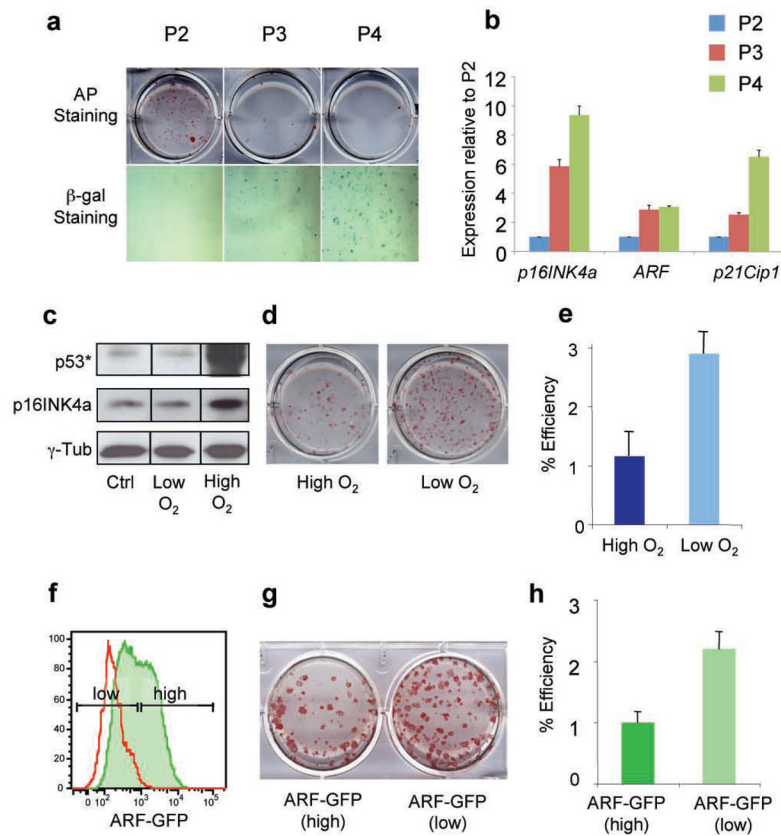


Figure 1. Reprogramming efficiency of fibroblasts is influenced by replicative potential and ARF expression status

(a) Alkaline phosphatase (AP) staining (top) of iPS cell colonies derived from secondary murine embryonic fibroblasts (MEFs) at different passages (P). Senescence associated β-galactosidase activity (bottom) of MEFs at same passages. (b) Expression levels of *p16INK4a*, *ARF* and *p21Cip1* in MEFs at the same passages as shown in (a). (c) Western blot analysis for p16INK4a and phospho-p53 (p53*) in MEFs grown at low (4%) or high (21%) oxygen. (d, e) Secondary MEFs grown under low O₂ give rise to iPS cells more efficiently. (f) ARF-GFP reporter MEFs (green line) at passage 3 show heterogeneous expression levels. Shown in red are wild type (WT) MEFs. (g, h) ARF-GFP^{low} MEFs give rise to transgene-independent AP⁺ iPS colonies more efficiently than ARF-GFP^{high} cells. Error bars depict the s.e.m.

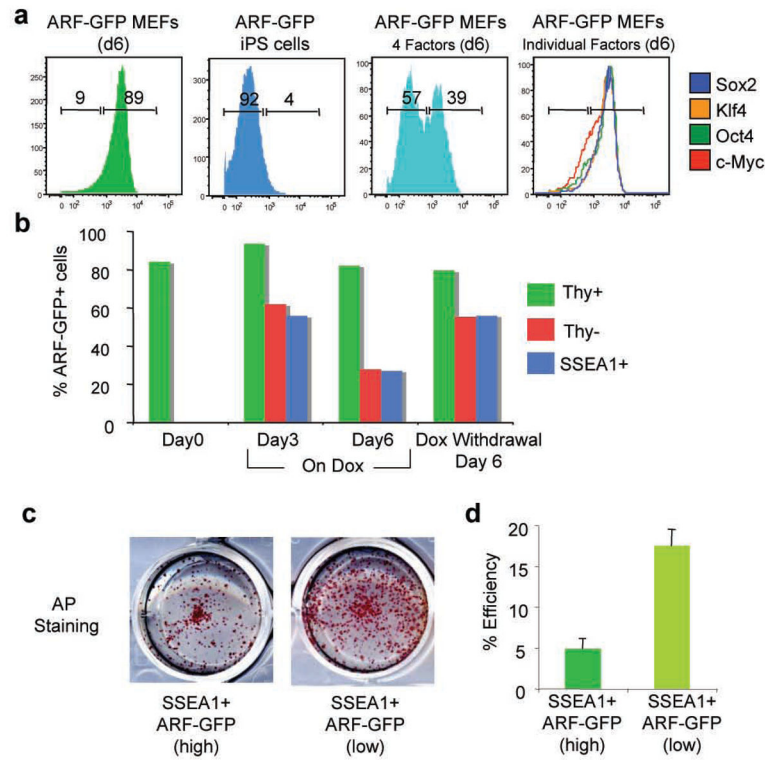


Figure 2. Transcription factor-induced downregulation of *INK4a/ARF* expression in cells undergoing reprogramming

(a) FACS plots of sorted ARF-GFP^{high} MEFs (first panel), established iPS cells from ARF-GFP MEFs (second panel), ARF-GFP^{high} MEFs expressing all four reprogramming factors (third panel) or each factor individually (last panel). (b) Time course of ARF-GFP expression in subpopulations of cells undergoing reprogramming. (c, d) ARF-GFP^{low} SSEA1⁺ cells at 6 days of transgene expression give rise to more transgene-independent AP⁺ iPS cell colonies than ARF-GFP^{high} SSEA1⁺ cells. Error bars depict the s.e.m.

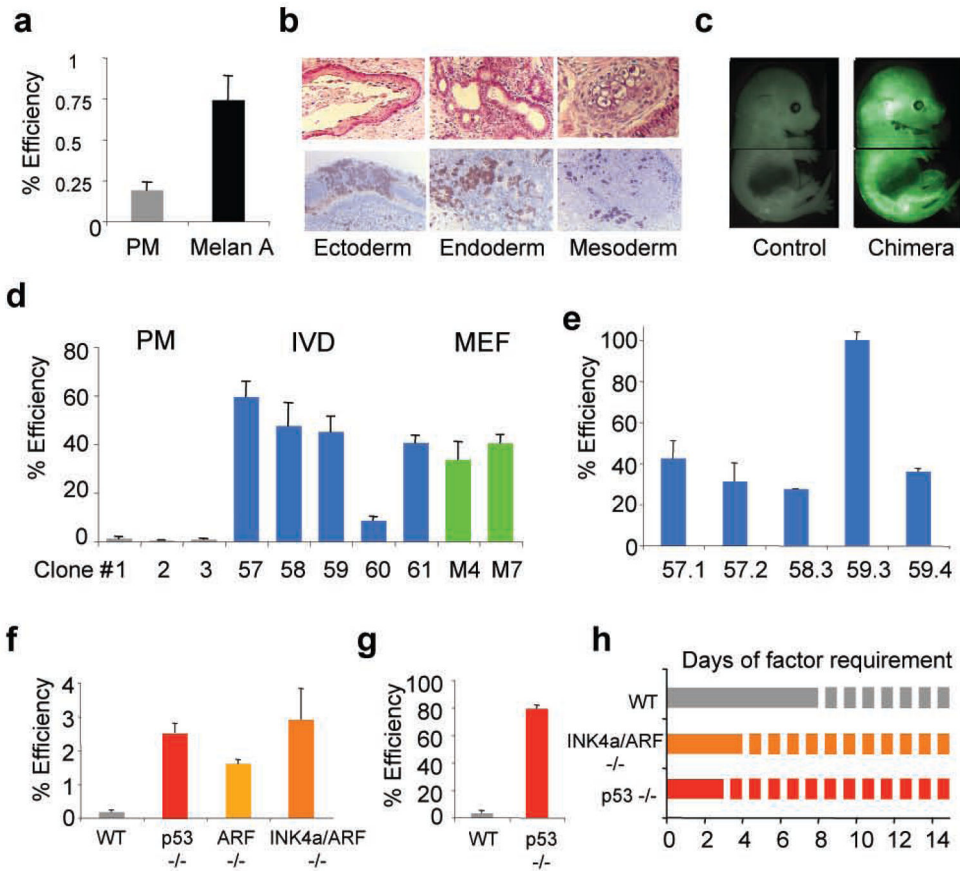


Figure 3. Cellular immortalization enhances reprogramming potential and kinetics
(a) Spontaneously immortalized Melan A cell line yields iPS colonies 3–4 times more efficiently than primary melanocytes (PM) upon direct viral infection. **(b, c)** Melan A-driven iPS cells show differentiation into ectodermal, mesodermal and endodermal derivatives in teratomas (b, top panel) and in chimeras produced from iPS cells labeled with a lentivirus constitutively expressing GFP (b, bottom panel, and c). **(d)** iPS cell formation efficiency of secondary (2°) cells derived from PMs (grey bars), Melan A-derived *in vitro*-differentiated (IVD) cells (blue bars) or Melan A-derived MEFs (green bars). **(e)** iPS cell formation efficiency of subclones of Melan A-derived IVD 2° cells. **(f)** Reprogramming efficiency of WT, p53 $^{-/-}$, ARF $^{-/-}$ and INK4a/ARF $^{-/-}$ MEFs upon direct viral infection. **(g)** Reprogramming potential of 2° p53 $^{-/-}$ iPS cell-derived E14.5 MEFs. **(h)** Evaluation of minimal temporal transgene requirement (solid lines) in WT, INK4a/ARF $^{-/-}$ and p53 $^{-/-}$ MEFs to form stable iPS cell colonies.

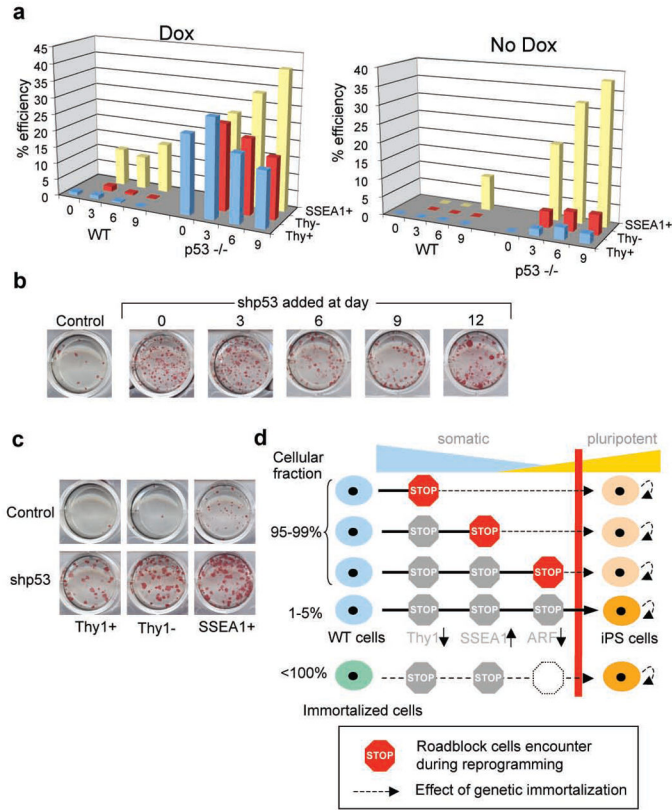


Figure 4. p53 deficiency rescues reprogramming potential in cells that normally fail to form iPS cells

(a) Comparison of reprogramming potentials of sorted Thy1⁺, Thy1⁻ and SSEA1⁺ subpopulations in WT and p53^{-/-} cells at different time points during reprogramming in the presence or absence of doxycycline (dox). (b) Acute inactivation of p53 by lentivirus expressing short hairpin (shp53) in secondary cells increases reprogramming efficiency at all time points. (c) Knockdown of p53 by shp53 rescues potential of Thy1⁻ and Thy1⁺ subpopulations to generate iPS cells. (d) Model summarizing the presented data; during factor-induced reprogramming, cells encounter different roadblocks such as the successful silencing of somatics genes (e.g., Thy1), the activation of pluripotency genes (e.g., SSEA1) and eventually the acquisition of immortality (e.g., silencing of ARF). The low efficiency of the process is likely due to the capacity of rare cells to overcome these roadblocks. In immortal fibroblasts, however, almost every cell is endowed with the potential to produce iPS cells. Moreover, cells that have already encountered a roadblock can be rescued by acute inactivation of p53 (indicated by dashed black lines). Red bar illustrates the transition point between somatic (blue) and pluripotent (yellow) state.